Paper presented at the Merton Flemings Symposium
MIT, Cambridge, Massachusetts – June 28-30, 2000
Proceedings edited by H. D. Brody et al. (TMS, Warrendale, PA, 2000)

STUDY AND MODELING OF HOT TEARING FORMATION

M. Rappaz[1], I. Farup[1,3] and J.-M. Drezet [1,2]

[1] Laboratoire de métallurgie physique
Ecole Polytechnique Fédérale de Lausanne
MX-G, CH-1015 Lausanne, Switzerland

[2] calcom SA, PSE, CH-1015 Lausanne, Switzerland

[3] SINTEF Materials Technology, P. O. Box 124 Blindern N-0314 Oslo, Norway

Abstract

As for most of the topics in the field of solidification, Mert Flemings has always pioneered new ideas. While much of the understanding of hot tearing formation was already known about 30 years ago, he devised with Metz an interesting equipment in order to study the resistance of mushy zones in compression and shearing [1,2]. Part of the results of these tests lead Flemings to be more and more interested in semi-solid processing of metallic alloys, with the success we know today (e.g., production of car components by thixocasting). Probably because of that, hot tearing criteria and models did not progress much since then. However, with the advent of refined stress and solidification models, one sees today a regain of interest for hot tearing. The present contribution, after recollecting some of the early work of Flemings in this area, presents recent SEM observations of hot tears in aluminum alloys and in-situ observations of hot tearing formation in organic systems. A recent model of hot tearing, which combines deformation of the mushy zone and interdendritic liquid flow, is also summarized.

1. Introduction

Hot tearing, a complex mechanism which involves deformation of the coherent and non-coherent solid skeleton as well as flow of the interdendritic liquid, follows also the "*first principle*" of solidification which basically states that : "*Whatever the topic you select in solidification, Mert Flemings has already worked on it and has outlined most of the underlying ideas*" ! About 30 year ago, Mert Flemings, in collaboration with S. Metz, devised an interesting shearing equipment in order to test the mechanical resistance of aluminum alloys in the semi-solid state [1,2]. They explained the influence of grain size, shearing rate, microstructure morphology, volume fraction of solid in terms of particles bonding/debonding, grain sliding and rearrangement. One of the first conclusions outlined in the second contribution [2] was that processing of metallic alloys in the semi-solid state should be feasible with various advantages. As a matter of fact, a very similar equipment has been used recently by St John and his group to study the initial rupture of semi-solid metals [3]. Along the same line, Mahjoub et al. have devised an axisymmetric shearing experimental set-up to study under well controlled conditions the breakage of particle bonds in aluminum alloys [4].

As Mert Flemings and his group focused their attention toward semi-solid processing, prediction of hot tearing did not progress much. For many years, the main criterion applied to characterize the Hot Cracking Sensitivity (HCS) of an alloy was based on the solidification interval [5] : the HCS increases with the width of the mushy zone. Feurer, maybe inspired by the work of Flemings and Piwonka on porosity [6], tried to derive a criterion based on the pressure drop of the interdendritic liquid, but only driven by solidification shrinkage [7]. Clyne and Davies [8], and much earlier Pellini [9], recognized the fact that hot tearing occurs in a critical region of the mushy zone where the film of interdendritic liquid is more or less continuous (i.e., brittle) and the permeability is low. They derived a HCS criterion based on a critical time spent by the mushy zone in the late stage of solidification.

More recently, we have derived a very simple model for HCS [10] similar to the Niyama criterion developed for porosity formation [11], but accounting also for strain-induced flow in the mushy zone. Although the model for the transition between the coherent and non-coherent regions of the mushy zone is fairly crude, it allows to determine the maximum strain rate that an alloy can sustain before a first pore nucleates. On the other hand, in-situ observations on organic alloys grown under Bridgman conditions and deformed in the transverse direction have allowed to directly visualize the formation of hot tears [12]. It was confirmed that hot tearing is indeed intergranular, that it occurs at a late stage of solidification and can be favored by the presence of pores. These in-situ observations have also allowed to better understand the presence of spikes in the ruptured surfaces of metallic alloys.

In Sect. 2 of the present paper, the work of Flemings and his group on hot tearing and early shear test experiments of aluminum alloys is further detailed. Recent SEM observations of hot tear surfaces of aluminum alloys are described in Sect. 3, whereas Sect. 4 presents in-situ observations of hot tearing formation in succinonitrile-acetone alloys [12]. Finally, the simple model of hot tearing formation recently published in [10] is summarized in Sect. 5 together some future developments.

2. Metz and Flemings' work

Most of the understanding of hot tearing formation was known at the end of the sixties, when Metz and Flemings started their work on mechanical testing of mushy zones [1,2]. From previous studies, it was quite clear that : i) hot tears form deep in the mushy zone where there is nearly a continuous film of liquid ; ii) hot tearing is induced by mechanical stresses of the coherent mushy zone underneath ; iii) grain refinement can decrease the hot cracking sensitivity ; iv) increasing the thermal gradient has two opposite effects : on one hand, it increases mechanical stresses and deformation of the coherent mushy zone, and on the other, it reduces the width of the mushy zone through which

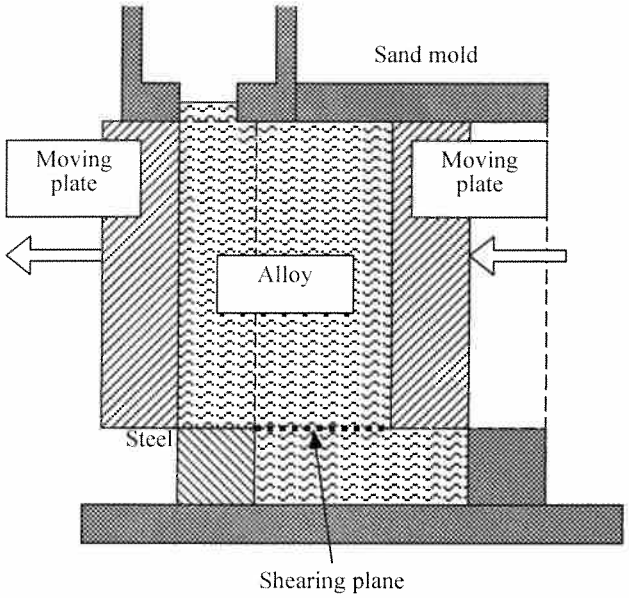

Figure 1 : *Schematics of the shearing test experiment developed by Metz and Flemings to study hot tearing [1,2].*

feeding of the liquid has to occur to compensate shrinkage and deformation.

Most of the previous studies on hot tearing had been made on test castings where stress was either allowed to develop naturally in specific configurations or eventually applied externally during cooling. The original idea of Flemings and Metz was to apply mechanically a well-defined compression or shearing to a well risered casting, isothermally at a known volume fraction of solid. The schematics of their experiment is reproduced in Fig. 1 for the shearing test only. In a sand mold, two vertical steel plates could move horizontally. In the case of compression test, one of the plate was fixed, whereas in the shear test, the two plates moved at the same speed but over only part of the height of the partially solid metal. The resistance of the mushy zone could be measured by strain gages, whose output was monitored on a visual recorder! The temperature, measured by a thermocouple inserted through the riser, was converted into a volume fraction of solid according to Scheil, but Flemings had outlined a few years before a back-diffusion model with Brody [13]. As mentioned in Sect. 1, St John and co-workers have used recently a very similar device to study the thixotropic behavior of aluminum alloys in the semi-solid state [3].

The many results Metz and Flemings found can be summarized as follows :

- In compression, the maximum stress that three different aluminum alloys could sustain was only a function of the volume fraction of solid, g_S, regardless of their composition (Al-4%Cu, Al-4%Si and Al-7%Si).
- In shear, the maximum true stress was a function of the volume fraction of solid, but also of the grain size. For the same value of g_S, the grain-refined specimen was weaker.

- In coarse-grain specimen, with well developed dendrites, they observe that the mushy zone develops some coherency at about $g_S = 0.25$, whereas this value is increased to about 0.4 for grain-refined specimens.
- Deformation can be partially accommodated by localized rearrangement of the grains at low volume fraction of solid, but no longer at $g_S > 0.5$.
- If the deformation is done at very low shear rate and high volume fraction of solid, strain accommodation by sliding of dendrites can deform the structure and in fact reinforce the resistance of the mushy zone. Tear is the result of progressive separation of dendrites to relieve stresses.

Although Metz and Flemings do not talk about coalescence of dendrite arms and strain localization at grain boundary, they already outlined most of the phenomena intervening in hot tearing. However, most of their conclusions were already oriented toward semi-solid processing and as a matter of fact, this was the first conclusion of their second paper [2]. Later, as Flemings became more interested in this later field, he abandoned that of hot tearing, which probably explains the absence of models if one excepts that of Clyne and Davies [8]. But a regain of interest for hot tearing has recently manifested, in particular in our institute [10,12], but also at other places [14,15].

3. Observations of hot tear surfaces

Scanning Electron Microscopy (SEM) investigations of hot tear surfaces in metallic alloys have already been made (see, e.g., References [5, 8]) and much of our knowledge in this field is based upon such studies. They all revealed the bumpy nature of hot tear surfaces, made of secondary dendrite arm tips, and clearly showed that hot tears form as interdendritic openings near the end of solidification. In some cases, phases having grown on the tear surface after the interdendritic opening can be observed. Analyzing these phases in the case of a commercial aluminium alloy, Nedreberg [16] confirmed that hot tears indeed form during the last stage of solidification. Spikes of a size of about 10 μm have been observed on the tear surfaces by Clyne and Davies [8], Spittle and Cushway [17], and recently by Drezet et al. [18]. These spikes are generally taken as evidences of solid bridges between the primary grains which have been elongated during hot tearing. However, as will be shown more clearly in the next section, these spikes can also be associated with the solidification of the last interdendritic liquid.

Spikes which formed on a hot-tear surface obtained in an alumininum–copper 3 wt.% alloy solidified on a cooled central cylinder (ring mould test, Ref. [18]) were further examined by SEM and stereo microscopy [12]. In one small region, the spikes shown in Fig. 2 were found.

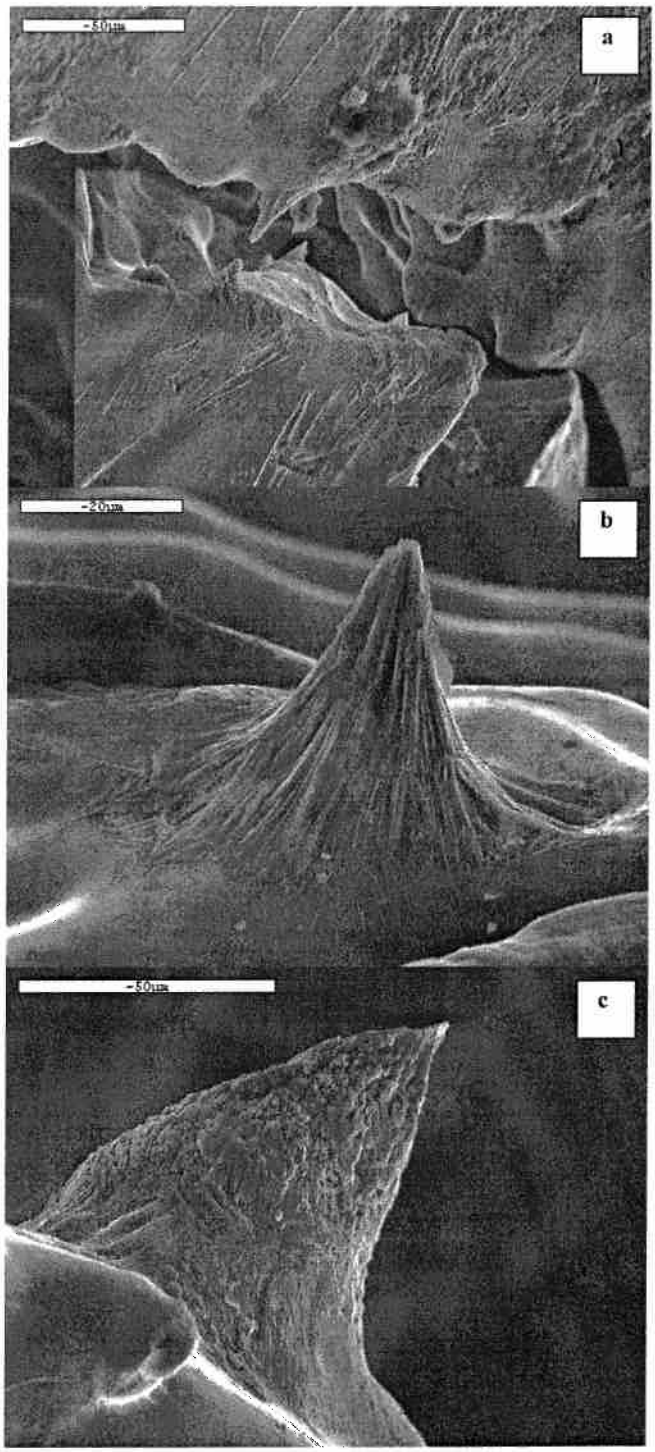

Figure 2 : *a) SEM observation of a hot tear in Al-3wt% Cu after having place the two sides of the crack facing each other. b) Drape-like spike probably formed by the last solidification of interdendritic liquid. C) Deformed spike probably formed by necking of a solid bridge .*

Whether spikes form by elongation and necking of solid bridges or by the solidification of last interdendritic liquid regions, it is expected that they should face each other on both sides of the hot tear surface. This is verified in Fig. 2(a) where the SEM views of both sides of a hot tear have been enlarged and placed in vis-a-vis. However, the appearance of the spikes may differ from one place to another as shown in the two enlarged SEM micrographs shown in Figs. 2(b) and 2(c).

In Fig. 2(b), the spike exhibits a characteristic "draped-looking" shape which is especially pronounced near the root. This might be what remains of an oxide layer on the liquid–gas interface. No traces of plastic deformation can be observed on these spikes, indicating that they are probably formed by the partial solidification of a last liquid bridge connecting two grains when these are pulled apart by mechanical stresses. This mechanism will be further detailed in the next section. Please note the bumpy appearance of the crack that can be seen behind this spike : it is associated with secondary dendrite arms and is typical of hot tears. It clearly indicates that most of the crack surface was covered with a nearly continuous liquid film at the time it formed.

In Fig. 2(c), another spike found in the same hot tear has a totally different morphology and is most probably due to the elongation and necking of a solid bridge formed prior to the opening of the crack. This spike exhibits a strongly deformed surface on the main part, but it has also a "draped-like" appearance at the root (especially on the left). Thus, it is most likely that this spike was also formed initially from a liquid meniscus across the grain boundary. However, this meniscus has solidified in such a way that the two solid parts coming from each side have coalesced before break-up of the liquid film. This solid bridge was subsequently deformed during further pulling.

These two spike formation mechanisms have been more clearly evidenced by the in-situ observations of organic alloys, as shown in the next section.

4. In-situ observations of hot tearing in organic analogs

Although *ex situ* investigations on as-tear surfaces abound, *in situ* observations of hot-tear formation are rare because of the technical problems involved with metallic alloys. Recently, Herfurth and Engler [19] developed a technique where an aluminium–copper alloy could be pulled apart during solidification between two silica–aerogel plates while directly observing. Unfortunately, their technique at the present stage only allows for the macroscopic study of crack formation at high temperature, and not really for hot tearing.

Due to its attractive properties such as transparency, low entropy of fusion, bcc lattice and convenient melting temperature, the succinonitrile (SCN)–acetone system has been used extensively in the past for in-situ observations of dendrite growth under stationary conditions [20,21]. The same experimental device has

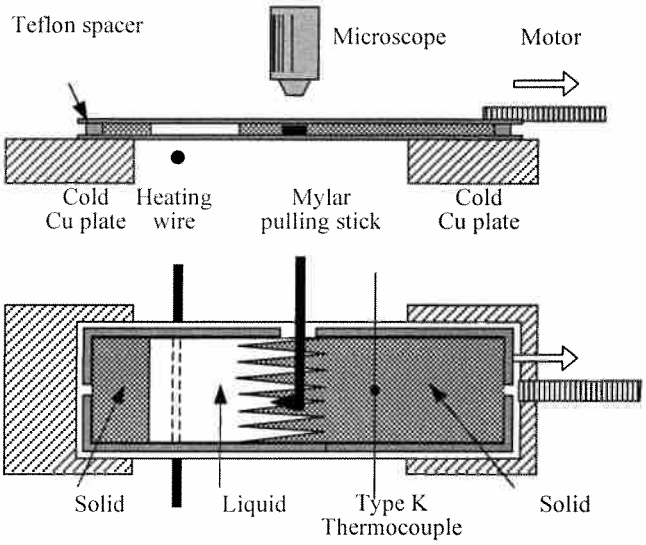

Figure 3 : *Schematics of the experimental device used to observe in-situ the formation of hot tears in succinonitrile-acetone alloys [12].*

been slightly modified recently in order to observe in-situ the formation of hot tears in such alloys. It is schematically described in Fig. 3.

Two glass plates (76 x 26 mm^2) are held apart by a rectangular 100-μm thick TEFLON frame spacer. For recording the temperature profile during the experiment and for determining the composition of the organic alloy, a type-K thermocouple with a wire diameter of 50 μm is inserted in the cell together with a pulling stick. This puller is used to deform the mushy zone perpendicularly to the growth direction. It is made of 100-μm thick MYLAR sheet. This material was selected for its strength sufficient to provide the pulling force, its thermal conductivity similar to that of SCN, and its adhesion to the solid SCN. After gluing the glass plates and spacer, the cell was filled by capillarity with the molten alloy.

The cell is then placed upon two water-cooled copper plates. Underneath the middle part of the cell, a resistance heating wire can remelt locally the alloy during the experiment. A motor and gear system ensures that the cell is moving at a constant speed in the thermal gradient supplied by this heating/cooling system. The experiments are performed in air and the solidification of the dendrites as well as the formation of hot tears can be observed through a microscope. The photographs shown in this paper are still pictures obtained from the video tapes recorded during the experiments by a video camera attached to the microscope.

After a rest period of about 30 min. to establish a thermal equilibrium between the heated wire and the cooled plates, the cell is moved at constant velocity. When the solidification front approaches the MYLAR puller, the puller is repositioned so that it is close to – but not across – a grain boundary (typical distance : 0.1–1 mm). Pulling is performed manually when the puller is

completely surrounded by solid material and the primary dendrites around the puller are more or less fully coalesced within a grain, but not at the grain boundary. Therefore, liquid only remains as a continuous film at the grain boundaries and as liquid pockets in between the coalesced dendrite arms. When pulling too early, liquid is able to fill the opening, whereas when it is too late, it becomes impossible to successfully open the network at a grain boundary, and the deformation is localized around the pulling stick.

Before presenting some micrographs, it should be pointed out first that in six of the cells, in which the amount of acetone was below 1.5 wt.%, hot tears could be initiated, whereas in the six other cells having higher solute concentrations, no tears could be initiated under similar pulling conditions. From this, a rough estimate of an upper limit of the liquid fraction for hot-tear formation in this system could be found assuming Scheil solidification (no diffusion of acetone in solid SCN). It was found that the remaining fraction of liquid when the tears form at the cold side of the mushy zone (30 °C) could be as high as 0.12 for a concentration of 1.5 wt.% of acetone (i.e., 0.88 volume fraction of solid). This result is somewhat higher than the value considered by Clyne and Davies for the "vulnerable" region of a mushy zone [8], but this result should be taken with some care since the present experimental conditions were not so accurately controlled (e.g., pulling was manual, levels of acetone and humidity in the cell was not carefully controlled).

A first example pertaining to the elongation and necking of a solid bridge is shown in Fig. 4. Dendrites are growing towards the left but their tips is quite far from the region where these three micrographs were taken. The lower edge of the pulling stick (A) appears white and the other optical contrasts seen in the solidifying alloy are coming from the interfaces between two media (e.g., solid-liquid, bubble-liquid, bubble-solid) connecting with the glass plates. Two grains can be distinguished in Fig. 4, the grain boundary (region labeled (B)) being nearly parallel to the side of the pulling stick. Within the grains, the dendrites arms are well coalesced but their structure can still be seen from the remaining liquid regions (wavy dark lines seen within the grains).

In Fig. 4(a), the pulling stick (A) has started to move slowly towards the top, thus opening the grain boundary (B) : as feeding is no longer possible deep in this region of the mushy zone, a tear has nucleated directly as a long pore on the grain boundary (B). The black lines/spots above and below the grain boundary are small pores which form between the glass plates and the solidified SCN-alloy – sometimes as a result of solidification shrinkage, but mainly due to the pressure drop associated with pulling.

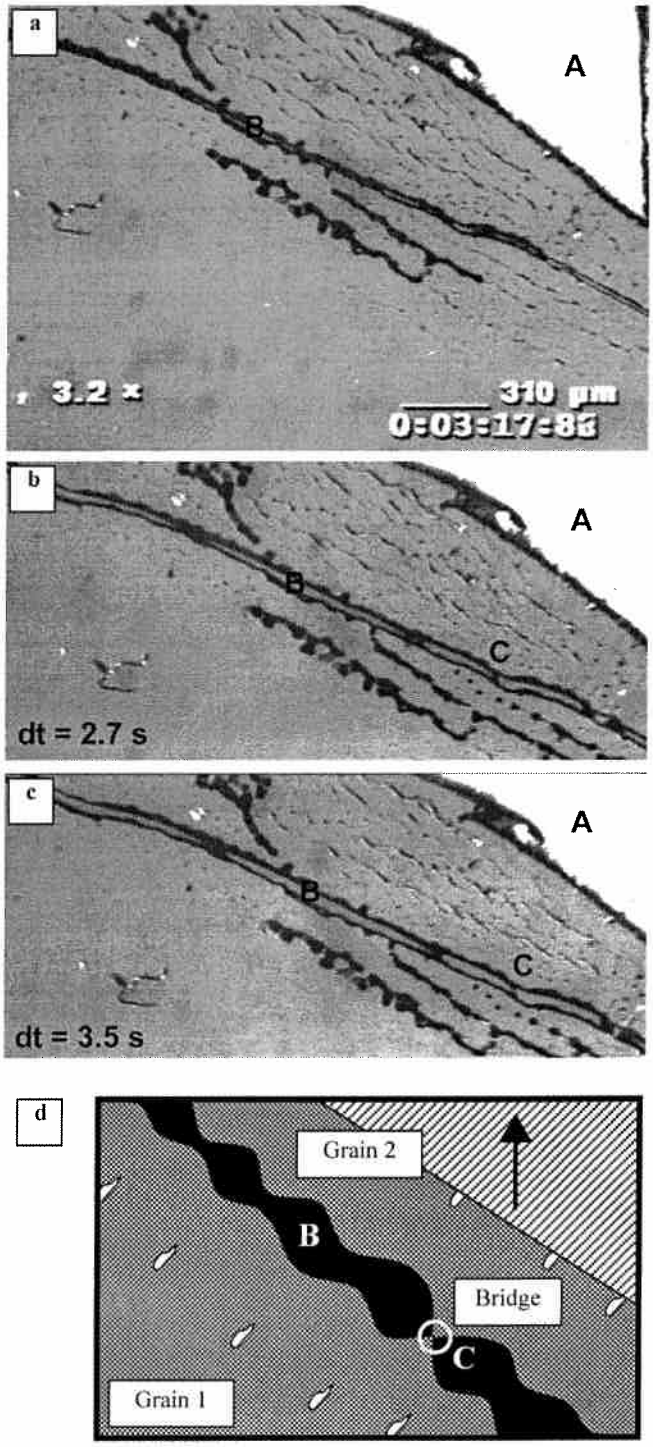

Figure 4 : *(a-c)Still images of a video sequence showing the formation of a hot crack in SCN-acetone at a grain boundary (B), with the stretching of a solid bridge leading to the formation of two spikes on each side of the crack (C). The pulling stick (A) is moved towards the top. The elapsed time since the beginning of the pull is indicated by dt and (d) is a schematic illustration of the bridge formation.*

As the pulling stick if moved further towards the top, the crack opens more (Fig. 4(b) taken 2.7 s after the beginning of the pull). It appears as a light gray opening (i.e., almost the same color as the solid dendrites !), but with a few black regions across the grains. These are regions where solid is connected, suggesting intergranular coalescence/bridging (see also the schematic diagram of Fig. 4(d)). These bridges appear black due to the fact that they do not fill entirely the space between the two glass plates, i.e., a small horizontal air gap exists between the solid and the glass plate. Upon further pulling (Fig. 4(c)), the bridge (C) of Fig. 4(b) is deformed and finally breaks up in two spikes facing each other (see also schematics shown in Fig. 4(d)).

Another interesting sequence of hot tear formation is shown in Fig. 5. During this sequence, two pores have nucleated at both extremities of a grain boundary (regions A and B in Fig. 5(a)). As the two grains are pulled further apart (Figs. 5(b) and 5(c)), the two pores grow while the interdendritic liquid in between nearly remains constant in volume but is stretched in the pulling direction (zone C). This situation is schematically represented in Fig. 5(h). As can be seen from the shape of the meniscus in Fig. 5(c), solidification has already started on the left side of the liquid bridge (non-spherical shape of pore A extremity), while it is still fully liquid on the right (spherical shape of pore B extremity). At this stage, the imposed separation between the two grains does not allow the fixed volume of liquid to maintain equilibrium conditions at the triple junction with the pore and the solid. Upon further pulling (Figs. 5(d-e)), the liquid part of the meniscus breaks away within a few hundredths of a second (Fig. 5(e-f)). While the solid part of the meniscus remains at the same location and finally gives two spikes on the two opposite surfaces of the hot tear (Fig. 5(f-g)), the remaining liquid sweeps around the solid part and quickly moves towards the left (Figs. 5(e-f)).

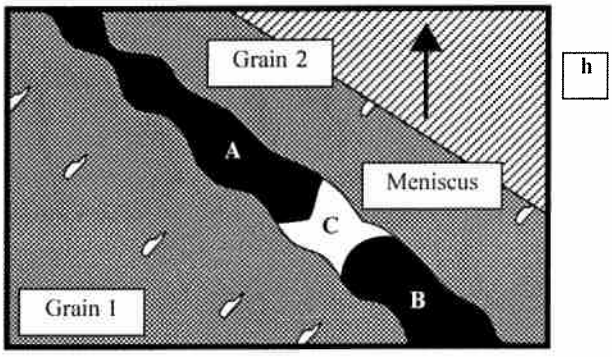

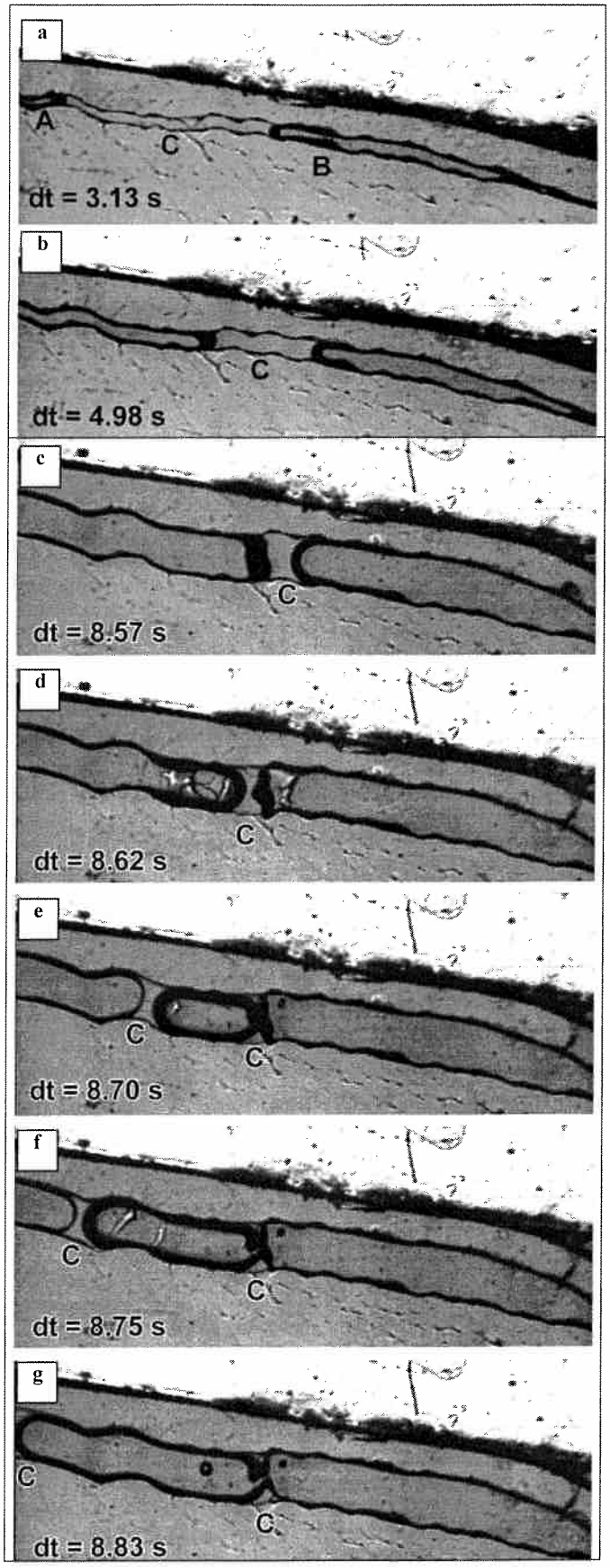

Figure 5 : *Still images of a video sequence showing the formation of a hot crack in SCN-acetone with the nucleation of two bubbles on both ends of a grain boundary (regions A and B). A small liquid meniscus (C) is trapped at the center. As the pulling stick (top) is moved towards the top, the meniscus is stretched until mechanical equilibrium can no longer be satisfied and disruptive breakage of the liquid film occurs, leaving two spikes on each side of the crack. A schematic illustration of this situation is shown above.*

It will settle in a narrower region of the hot tear (not shown in these pictures),where mechanical equilibrium can again be established between the capillary forces.

Although the sequences of events shown in Figs. 4 and 5 for SCN-alloys are certainly influenced by the presence of the two glass plates and the high vapor pressure of acetone (and possibly water), similar mechanisms in metallic systems probably occur, thus offering a plausible explanation for the spike morphology observed ex-situ in such systems (Sect. 3).

5. A new model for hot tearing

From the experimental findings shown in Sects. 3 and 4 and of previous research, it is clear that hot tearing form : (i) at grain boundaries where coalescence of dendrite arms is made difficult due to grain boundary energy ; (ii) deep in the mushy zone where liquid feeding is difficult ; but (iii) just ahead of the fully coalesced regions where there is still a nearly-continuous film of interdendritic liquid at the grain boundaries and thermomechanical strains can be easily transmitted from the fully coherent dendritic network underneath.

Therefore, hot tearing formation can be schematically described by Fig. 6 for a nearly steady-state situation (i.e., Bridgman growth conditions) [10]. Columnar dendrites are assumed to grow in a given thermal gradient, G, and with a velocity, v_T, equal to the speed of the liquidus isotherm. This velocity points towards the top and therefore, the liquid has to flow from top to bottom in order to compensate for shrinkage, the specific mass of the solid being larger than that of the liquid for most metallic alloys. Dendrite arms belonging to the same grain have coalesced since there is no grain boundary energy to overcome. At some grain boundary, the permeability of the mushy zone is greater, and thus interdendritic liquid can flow more easily, but at the same time, dendrite arms have not yet coalesced due to the grain boundary energy. This last contribution is clearly dominating hot tearing formation.

If the dendritic network is submitted to a tensile deformation rate, $\dot{\varepsilon}_p$, perpendicular to the growth direction, the flow of liquid should also compensate for that deformation if hot tears are to be avoided. As can be seen in Fig. 6, strain localization is likely to happen at the grain boundary since this is the weakest part of the mushy zone [5]. Let now consider the pressure in the interdendritic liquid : it decreases from the metallostatic pressure, p_m, near the dendrite tips to some lower values, p_{min}, at the roots (gravity is neglected for the sake of simplicity). If the pressure falls below a cavitation pressure, p_c, at the grain boundary, a void may form (black region in Fig. 6 surrounded by a small rectangle), and then can propagate into a crack, providing the stresses are not released. Therefore, as introduced in [10], a hot tear will form if the critical pressure is reached at the roots of the dendrites :

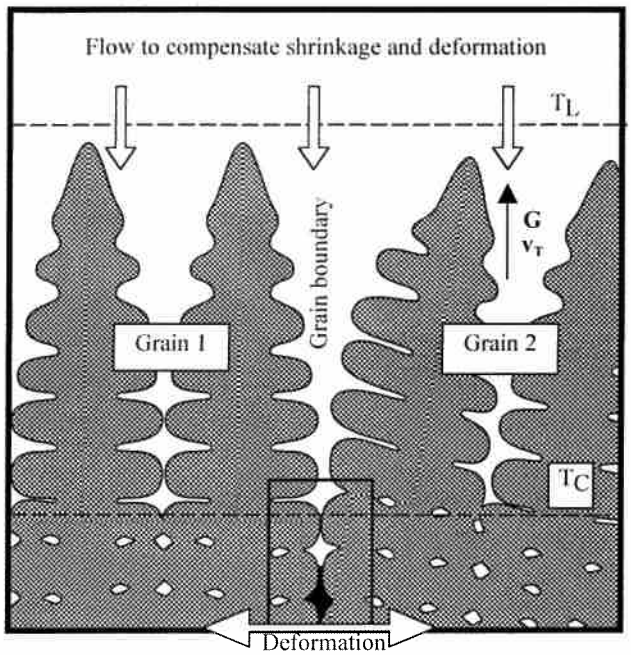

Figure 6 : *Schematics of the mushy zone under columnar growth conditions showing the transition between the coherent and incoherent regions (at temperature T_C), the grain boundary remaining with a continuous film of liquid. The interdendritic flow has to compensate for shrinkage and deformation (in this case assumed to be transverse to the thermal gradient). A hot tear forms at the grain boundary.*

$$p_{min} = p_m - \Delta p_\varepsilon - \Delta p_{sh} = p_c \qquad (1a)$$

or

$$\Delta p_{max} = \Delta p_\varepsilon + \Delta p_{sh} = \Delta p_c = p_m - p_c \qquad (1b)$$

Δp_ε and Δp_{sh} are the pressure drop contributions associated with deformation and shrinkage, respectively (taken as positive values). In order to calculate these two contributions, a mass balance is performed at the scale of a small volume element (see [10] for details). In a reference frame attached to the isotherms and under steady state conditions, this mass balance can be written as:

$$\mathrm{div} \langle \rho \mathbf{v} \rangle - v_T \frac{\partial \langle \rho \rangle}{\partial x} = 0 \qquad (2)$$

where the notation "<.>" is used to indicate values locally averaged over the liquid and solid phases. The average specific mass $\langle \rho \rangle = \rho_S g_S + \rho_l g_l$ is the mean specific mass of the solid and liquid phases and $\langle \rho \mathbf{v} \rangle = \rho_S g_S \mathbf{v}_S + \rho_l g_l \mathbf{v}_l$ is the average mass flow. The volume fraction of liquid, g_l, is equal to $(1 - g_S)$ and the specific masses of the two phases, ρ_S and ρ_l, are assumed to be constant, but not equal. Considering that the fluid moves along

the x-axis only, whereas the solid deforms in the transverse direction, one has :

$$\frac{\partial(\rho_l g_l v_{l,x})}{\partial x} + \frac{\partial(\rho_S g_S v_{S,y})}{\partial y} - v_T \left[\frac{\partial(\rho_S g_S)}{\partial x} + \frac{\partial(\rho_l g_l)}{\partial x} \right] = 0 \qquad (3)$$

Taking g_S as a function of x only, Eq. 3 can be rewritten in the form :

$$\frac{d(g_l v_{l,x})}{dx} + (1+\beta)\, g_S \dot{\varepsilon}_p - v_T \beta \frac{dg_S}{dx} = 0 \qquad (4)$$

where the deformation rate of the solid along the y-direction :

$$\dot{\varepsilon}_p = \frac{\partial v_{S,y}}{\partial y} \qquad (5)$$

has been introduced, together with the shrinkage factor :

$$\beta = \frac{\rho_S}{\rho_l} - 1 \quad (\beta > 0). \qquad (6)$$

The integration of Eq. 4 over the distance x gives :

$$g_l v_{l,x} = -(1+\beta)\, E(x) - v_T \beta g_l \qquad (7)$$

where E(x) is the cumulated deformation rate defined as :

$$E(x) = \int g_S \dot{\varepsilon}_p dx \qquad (8)$$

In the absence of deformation (E = 0), it is interesting to note that the actual velocity of the fluid, $v_{l,x}$, is constant and equal to $-v_T\beta$ at any point of the mushy zone. This was already established by Niyama for the formation of porosity [11].

On the other hand, if one considers that the thermal strain induced by the coherent mushy zone underneath is localized at grain boundaries while the inner part of the grains is not deformed, a factor must be introduced in the strain rate term of Eq. (7). Although it is difficult to estimate because of the complex rheology of the transition from coherent to incoherent regions, it could be written near a grain boundary as :

$$\dot{\varepsilon}_p = \frac{\phi}{\lambda} \langle \dot{\varepsilon}_p \rangle \qquad (9)$$

In this equation, ϕ is typically the grain size (in the direction perpendicular to the thermal gradient if this is a columnar structure), λ is proportional to the "width" of the grain boundary where strain is localized (e.g., of the order of the secondary dendrite arm spacing) and $\langle \dot{\varepsilon}_p \rangle$ is an average strain rate deduced at the level of the coherency temperature from a continuous mechanical model.

The LHS term of Eq. 7 can be related to the pressure gradient in the liquid via the Darcy equation [6,10,11]:

$$g_l v_{l,x} = -\frac{K}{\mu} \frac{dp}{dx} \qquad (10)$$

where K is the permeability of the mushy zone and μ the viscosity of the liquid. Please note that the contribution of gravity has been neglected in this equation. Combining Eqs. 7 and 10 and integrating over the whole length of the mushy zone finally gives the pressure drop between the tips and roots of the dendrites :

$$\Delta p_{max} = \Delta p_\varepsilon + \Delta p_{sh} = (1+\beta)\mu \int_0^L \frac{E}{K} dx + v_T \beta \mu \int_0^L \frac{g_l}{K} dx \qquad (11)$$

At this stage, Eq. (11) is quite general and can be easily extended to non steady-state situations. Setting up a cavitation pressure (Eq. (1)), it gives the maximum strain rate (or value of E) that the mushy zone can sustain before a hot tear nucleate. It should be pointed out that, under steady-state conditions, the integration over x can be replaced by an integration over the temperature, thus introducing the thermal gradient and the solidification interval of the alloy [10]. Assuming that the permeability is given by the Carman-Kozeny relationship [6,10,11], the maximum strain rate, $\dot{\varepsilon}_{p,max}$, associated with a given alloy and cavitation pressure is given by :

$$F(\dot{\varepsilon}_{p,max}) = \frac{\lambda_2^2}{180} \frac{G}{(1+\beta)\mu} \Delta p_c - v_T \frac{\beta}{1+\beta} H \qquad (12)$$

λ_2 is the secondary dendrite arm spacing, G is the thermal gradient, and F and H two contributions given by :

$$F(\dot{\varepsilon}_p) = \int_{T_S}^{T_L} \frac{E(T)\, g_S(T)^2}{(1 - g_S(T))^3} dT \qquad (13)$$

$$H = \int_{T_S}^{T_L} \frac{g_S(T)^2}{(1 - g_S(T))^2} dT \qquad (14)$$

Setting a value to Δp_c, Eq. (12) allows to determine $\dot{\varepsilon}_{p,max}$ providing : (i) the solidification path, $g_S(T)$, is known, and (ii) the transmission of the strains from the coherent to the non-coherent parts of the mushy zone, i.e., the dependence $\dot{\varepsilon}(x)$ or $\dot{\varepsilon}(T)$, is given. The first contribution can be determined via a microsegregation model, such as the Brody-Flemings equation [13]. The second point is more delicate, as stated previously, but one can for example assume that $\dot{\varepsilon}(T)$ is uniform along the x direction (i.e., the two grains at the boundary move with a lateral displacement which is uniform). Finally, the integration of Eqs (13) and (14) has to be performed until coherency is reached at the grain boundary, which is another unknown of the problem. According to the work of Clyne and Davies [8] and to the observations made on organics [12], T_S can be set to T_E if more than 2% eutectics form in the alloy. Otherwise, T_S can be fixed to the temperature at which g_S reaches a critical value (in this case 0.98 volume fraction of solid).

Keeping these points in mind, the value $\dot{\varepsilon}_{p,max}$ obtained from Eq. (12) for of a given alloy and cavitation pressure allows to define a HCS index as :

$$HCS = (\dot{\varepsilon}_{p,max})^{-1} \quad (15)$$

This HCS index, normalized between zero and unity, was calculated for the two thermal conditions defined by Clyne and Davis [8]: mode 1 corresponds to a constant cooling rate, $\dot{T}$, and mode 2 to a constant rate of heat extraction, $\dot{H}$, ($\dot{H} = c_p\dot{T} - L\dot{g}_S$, where c_p and L are the specific heat and latent heat of fusion, respectively). The cavitation depression, Δp_c, was set to 2 kPa, a value which is on the order of that deduced from porosity modeling in Al-Cu alloys [22]. The resulting HCS index is compared in Fig. 7 with the measurements of Spittle and Cushway for different compositions, c, of non grain-refined Al-Cu alloys [17]. These authors have used "dog-bone" shape cylindrical molds to cast these alloys. The electrical resistance of the specimens was then measured after solidification and converted into a HCS index varying from 0 to 1. Also reported in Fig. 7 are the Clyne and Davis criterion for modes 1 and 2 and a criterion which is simply proportional to the solidification interval of the mushy zone (including back-diffusion).

The Λ-shape curve, typical of hot tearing, is well reproduced by the present criterion for both modes : the rapid increase at low solute content and the maximum at a composition of around 1.4 wt. pct Cu predicted by the criterion are in relatively good agreement with the measurements of Spittle and Cushway. Please note that the maximum of the HCS curves is very close to the maximum of the solidification interval as pointed out by Campbell [5]. The decrease between 1.4 and 3% is somewhat too steep in the present model but the vanishing values obtained at concentrations higher than 3% are again close to the experimental ones. On the other hand, the criterion of Clyne and Davis for mode 1 surprisingly does not reproduce the increase of the HCS at low concentration and was discarded by these authors. The same criterion computed for mode 2 yields a too wide Λ–curve and overestimates the HCS values as compared with experiments, especially at higher concentrations. Finally, the model based simply on the solidification interval predicts a far too slow decrease past the maximum.

It should be pointed out that the measurements of Spittle and Cushway correspond to an overall cracking length of the specimens : their HCS index is therefore an indication of the *propagation* of hot tears. The present model is only a criterion for the *appearance* (initiation) of the first hot tear in the interdendritic liquid and not of its propagation. However, in the steady state conditions considered in the present model, there are no reasons for an initiated hot tear to stop propagating unless the deformation rate decreases.

A few remarks can finally be made :

- The fraction of solid at which interdendritic bridging is assumed to occur (0.98) has a great influence on the position of the peak of the Λ–curves : when this value tends toward unity, the concentration of the HCS maximum tends toward zero. This is due to the singularity of the permeability function when $g_S \rightarrow 1$. Bridging of dendrite arms (or coalescence) has not been study in solidification and further work is needed in this area, both from an experimental point of view (e.g., observation in organic alloys [12]) and modeling (e.g., using a multiphase field approach [23]).
- Strain localization (Eq. (9)) has not been accounted for in the results of Fig. 7. As know experimentally, coarse-grained specimens are more prone to hot tearing simply because ϕ is increased in Eq. (9). In other words, for a given value of $\dot{\varepsilon}_{p,max}$ that the mushy zone (or a grain boundary) can sustain before giving a crack, the actual value calculated from a continuous stress model, $\langle\dot{\varepsilon}_{p,max}\rangle$, is reduced when the grains are coarse. Please note that for fine grain specimens, the structure is no longer dendritic and difficulty arises in defining "a" thickness of the grain boundary, λ_2, where strain localization occurs.
- Finally, the transition between coherent and non-coherent regions of the mushy zone is certainly gradual as seen from the spikes formation (Sects. 3 and 4). This means that the "resistance" to opening of a given grain boundary is not

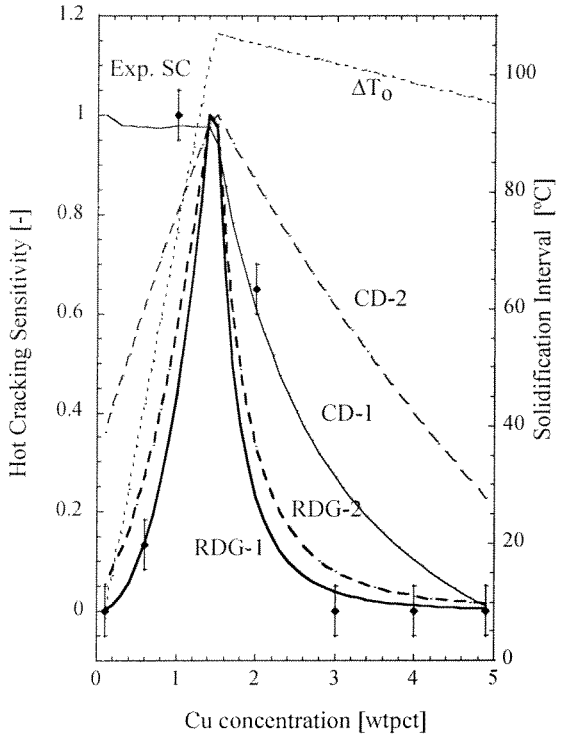

Figure 7 : *Hot-Cracking Sensitivity calculated for aluminum-copper alloys as a function of Cu concentation. RDG : model of Rappaz et al. [10] ; CD : model of Clyne-Davis [8] ; 1 : constant cooling rate ; 2 : constant heat extraction rate ; ΔT_0 : solidification interval. The points correspond to the measurements of Spittle and Cushway [17].*

only Δp_c in the non-coherent region. Macroscopic stress calculations could be performed with a gradual decrease of the mechanical properties ahead of the coherency temperature as a function of the percentage of dendrite arms which have bridged. However, it appears from the in-situ observations on organics and from the spike morphologies in metallic alloys, that nucleation of hot tears starts usually *before* solid bridges are established across the gap. The resistance of such liquid bridges which are stretched across an opening crack is of the order of $(\gamma\, 2\pi R\, n_A)$, where γ is the liquid-gas interfacial energy (about 1 N/m), R the radius of a bridge (i.e., the radius of the root of a conical spike, about 10 μm) and n_A is the density of bridges across a crack surface. The pressure resistance offered by as many as 1 liquid bridge every $100 \times 100\ \mu m^2$ of crack surface (i.e., $n_A = 10^8\ m^{-2}$) is of the order of the cavitation pressure set in the present calculations.

Conclusion

As in many area of solidification, Flemings and his group at MIT has initiated new ideas which still outline many of the current researches done today, either experimentally or with the help of increasingly powerful computers. In his attempt to understand, and possibly model, hot tearing formation about thirty years ago, his attention (fortunately or not, the question is open !) was diverted rather towards semi-solid processing !

Hot tearing is certainly a very complex phenomenon since it is at the frontier between fluid dynamics and solid deformation. Although the model presented here is fairly simple, it captures some of the physics that was known before but not explicitly written. The coalescence or bridging of dendrite arms within a grain and at grain boundaries is a key parameter in defining coherency in tensile or shearing testing. It is also a key parameter in semi-solid processing. Yet, this topic has been totally ignored up to now and will need to be addressed in the future in order to better understand agglomeration of particles in semi-solid processing and mechanical resistance during hot tearing formation.

References

1. S. A. Metz and M. C. Flemings, AFS Trans. **77** (1969) 329.
2. S. A. Metz and M. C. Flemings, AFS Trans. **78** (1970) 453.
3. H. Wang, D. H. St John, C. J. Davidson and M. J. Couper, in *Solidification and Gravity 2000*, eds. A. Roosz et al (Materials Sc.Forum Vols. 329-330, 2000) p. 449.
4. K. Mahjoub, A. Mortensen and M. Rappaz, *Semi-solid shear behavior of A356 Al alloys at the onset of breakage*, submitted to the Semi-Solid Conference (Torino, 2000).
5. J. Campbell, *Castings* (Butterworth-Heinemann, Oxford, 1991).
6. T. S. Piwonka and M. C. Flemings, Trans. AIME **236** (1966) 1157.
7. U. Feurer, Giesserei Forsch. **2** (1976) 75.
8. T. W. Clyne and G. J. Davies, Brit. Found. **74** (1981) 65.
9. W. S. Pellini, Foundry (Nov. 1952) p. 125.
10. M. Rappaz, J.-M. Drezet and M. Gremaud, Met. Mater. Trans. **30A** (1999) 449.
11. E. Niyama, T. Uchida, M. Morikawa and S. Saito, AFS Int. Cast Metals J. (Septembre 1982) 52.
12. I. Farup, J.-M. Drezet and M. Rappaz, *In-situ Observation of Hot Tearing Formation in Succinonitrile–Acetone*, Mater. Sc. Engng. (submitted).
13. H. D. Brody and M. C. Flemings, Trans. AIME **236** (1966) 615.
14. I. Farup and A. Mo, *Two-Phase Modelling of Mushy Zone Parameters Associated with Hot Tearing*, Met. Mater. Trans. (2000) to appear.
15. W. M. Van Haften, W. H. Kool, L. Katgerman, Mater. Sc. Forum, **331-337** (2000) 265.
16. M. L. Nedreberg. PhD thesis, University of Oslo, Dept. of Physics, February 1991.
17. J. A. Spittle and A. A. Cushway, Metals Technology, **10** (1983) 6.
18. J.-M. Drezet, O. Ludwig, and M. Rappaz. In *Mecamat* (French Society of Metallurgy, Y. Berthaud, editor, 1999) p.30.
19. Th. Herfurth and S. Engler. In *Erstarrung metallischer Schmeltzen in Forschung und Gießereipraxis*, A. Ludwig, editor, (DGM, Oberursel, 1999) p. 37.
20. R. Chopra, Met. Trans., **19A** (1988) 3087 ; J. Cryst. Growth, **92** (1988) 543.
21. H. Esaka, W. Kurz and R. Trivedi, in *Solidification Processing*, Eds. J. Beech and H. Jones (Inst. Metals, London, 1988) p.198.
22. J. Ampuero, Ch. Charbon, A. F. A. Hoadley and M. Rappaz, in *Materials Processing in the Computer Age*, Eds. V. R. Voller, M. S. Stachowicz et B. G. Thomas (TMS Publ., Warrendale, Pennsylvania, 1991), p.377-388.
23. A. Soguel, EPFL diploma work (2000).